International Journal of GEOMATE, Oct., 2022, Vol.23, Issue 98, pp.109-116
ISSN: 2186-2982 (P), 2186-2990 (O), Japan, DOI: https://doi.org/10.21660/2022.98.3518
Geotechnique, Construction Materials and Environment

# GRAVITY INVERSION MODELLING USING SIMULATED ANNEALING AND THE LEVENBERG-MARQUARDT ALGORITHM

* Agus Setyawan [1], Muhammad Kautsar Aqsa[1], Jatmiko Endro Suseno[1] and Rina Dwi Indriana[1]

[1] Physics Department, Faculty of Science and Mathematics, Diponegoro University, Semarang, Indonesia

*Corresponding Author, Received: 14 July 2022, Revised: 30 Sept. 2022, Accepted: 10 Oct. 2022

**ABSTRACT:** The gravity method is a geophysical method that can model subsurface conditions based on variations in density. This model can be obtained by performing a mathematical computation process of gravity data which is known as the inversion modeling process. During its development, inversion modeling solutions can be obtained with local and global approaches. A comparison of the two approaches was carried out, namely using the Levenberg-Marquardt (LM) algorithm for the local approach and the simulated annealing (SA) algorithm for the global approach. The research begins with the study of synthetic data horizontal block, vertical block, and faults models. From the synthetic study, both algorithms were rated good based on an average root mean square error (RMSE) value of 0.03 mGal with a correlation of 76% for the LM algorithm and an average RMSE of 0.6 mGal with a correlation of 61% for the SA algorithm. The two algorithms were also tested on the Ungaran geothermal field gravity data. RMSE value was 0.001 mGal for the LM algorithm and 0.7 mGal for the SA algorithm due to the field data test. The two models produced by each algorithm are assessed to be correlated with geological information and models in previous studies.

*Keywords: Density, Inversion modeling, Gravity inversion, Simulated annealing, Levenberg-Marquardt*

## 1. INTRODUCTION

Geophysical exploration aims to create subsurface models by relying on measured field data [1]. The subsurface physical parameter model can be obtained by applying a mathematical computation technique to the measurement data which is called inversion modeling. Inversion modeling produces a more efficient quantitative solution than the trial-and-error approach of forwarding modeling [2]. The problem that often arises in gravity data modeling is ambiguity, that is the same gravity response can be generated from different models. Researchers continue to try to develop inversion modeling techniques that produce the best models.

The inversion modeling method that is commonly used in gravity data is the least-square algorithm [3]. This algorithm often overfits noise data [4]. Some researchers modify the least-square by including the damping parameter $\lambda$ and determining the value change rule which is expected to solve the overfitting problem [5,6]. This rule was further developed by [7] and is known as the Levenberg-Marquardt (LM) algorithm. The LM algorithm is considered good enough for non-linear problems including the magnetotelluric (MT) method [8,9], moreover, in this stud,y it will be observed whether this algorithm can also work well on linear (gravity) problems.

Simulation annealing (SA) is a random search algorithm that was popularized by [10]. SA is a very flexible algorithm because it can find solutions to both linear and non-linear problems [10]. This algorithm also excels in computational effectiveness because it does not require the calculation of derivatives and inverses of large matrices [11]. Some of these studies use SA to inverse 1-dimensional MT models [10,11], therefore, the application of SA in the case of 2-dimensional gravity is deemed necessary, so that it can be determined whether this directional random search algorithm can produce a good result. Simulated annealing has been applied to the gravity method inversion modeling by [12] and [13], and ato for the MT method by [9]. The objective of this research is to observe how the performance of the LM algorithm which looks for a solution based on the principle of regression compared to the SA algorithm which looks for a solution based on directional random search in solving the 2-dimensional gravity inversion problem.

## 2. RESEARCH SIGNIFICANCE

Geothermal energy is feasible renewable energy to be an alternative to fossil energy which can harm the environment if used in large quantities continuously. Research in the development of geothermal exploration technology continues to be carried out, especially in the field of geophysics. Geophysical subsurface structure modeling is an important part of geothermal exploration. This modeling can affect the accuracy of the drilling point which leads to the cost efficiency of

exploration. Thus, it is necessary to research the development of geophysical modeling algorithms.

## 3. METHOD

### 3.1 Gravity Modelling

The gravitational modeling of the earth can be discretized by several prisms as shown in Fig. 1 [14]. Gravity anomalies of continuous 2D objects that are discretized are mathematically written by [15] and modified by [14] as in Eq. (1).

$$g = 2\gamma\rho \sum_{n=1}^{N} \frac{\beta_n}{1+\alpha_n^2}\left[log\frac{r_{n+1}}{r_n} - \alpha_n(\theta_{n+1} - \theta_n)\right] \quad (1)$$

g is the gravity anomaly at the point observed, γ is the gravitational constant, ρ is the prism density and $\theta_n$ is the angle between the distance of an observed point to the prism the and horizontal distance. $\beta_n$ and $\alpha_n$ are the geometrical factors explained mathematically in Eq. (2) and (3).

$$\alpha_n = \frac{x_{n+1}-x_n}{z_{n+1}-z_n} \quad (2)$$

$$\beta_n = x_n - \alpha_n z_n \quad (3)$$

With $x_n$ and $z_n$ being the horizontal and vertical distance from an observed point to the object.

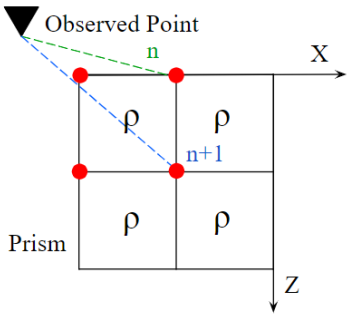


Fig.1 Earth discretization to a 2D prism

### 3.2 Levenberg-Marquardt (LM) Algorithm

The Levenberg-Marquardt (LM) algorithm is a linear approach to solving non-linear problems [7]. The LM algorithm adds the damping parameter λ to prevent overfitting. The addition can be written as Eq.(4) [11].

$$m_{n+1} = m_n + J_n^T\,[\,J_n J_n^T + \lambda I]^{-1}\,(d - K(m_n)) \quad (4)$$

Geometric information needs to be added to the calculation of the model and has been modified by [16], it can be written mathematically in Eq. (5) and (6).

$$m_{n+1} = m_n + W_n^{-1}\,J_n^T\,[\,J_n\,W_n^{-1}\,J_n^T\lambda I]^{-1}\,(d - K(m_n)) \quad (5)$$

Wn is the weighting matrix in which the diagonal elements can be written as Eq. (6).

$$W_{jj}^n = \frac{R_{ij}^2}{m_j^n+\varepsilon} \quad (6)$$

$R_{ij}^2$ is the minimum distance from observation point i to the prism, j and $\varepsilon$ are positive` numbers with the order of $10^{-7}$ to avoid errors due to division by 0 (zero).

### 3.3 Simulated Annealing Algorithm

The simulated annealing (SA) algorithm is based on crystal annealing events when the minimum energy is reached. This algorithm performs a directional random search for solutions (each perturbation has a different chance of being accepted into the solution). The application of annealing in the case of inversion can be described mathematically as Eq. (7) [10].

$$P = \exp\left(-\frac{\Delta E}{kT}\right) \quad (7)$$

*P* is the probability, *E* is the objective function, *k* is the Boltzmann constant and *T* is the controlling factor. The Model space must be determined empirically. Model perturbation is taken randomly as an arbitrary number in the model space using Eq. (8) [3].

$$m_{i+1} = m_i + R\left(m^{max} - m^{min}\right) \quad (8)$$

*R* is a random number selected from the model space. The final stage is to apply a constant decrease of the control factor *T* to obtain a minimum objective function. The quality of the model can be assessed from the root mean square error (RMSE) and the correlation (*r*) calculated using Eq. (9) [17] and Eq. (10) [18].

$$RMSE = \sqrt{\frac{1}{N}\sum_{i=1}^{N}(K(m_i) - d_i)^2} \quad (9)$$

$$r = \frac{N\sum xy - (\sum x)(\sum y)}{\sqrt{(N\sum x^2 - (\sum x)^2)(N\sum y^2 - (\sum y)^2)}} \quad (10)$$

*N* is the number of gravity data, *K* is the forward operator, mi is the ith model, and di is the ith gravity data used in this study are the synthetic data and gravity data of Mount Ungaran that were obtained from the study of [19]. The data was processed with Python 3.7. This research is divided into 2 stages,

which are synthetic data studies and field data studies. Variations of synthetic models used are horizontal z, vertical block and fault models. The geometric information used are the depth boundary from spectrum analysis and the horizontal boundary from the horizontal gradient analysis. There are several algorithms to implement SA, this study uses the metropolis algorithm. The misfit tolerance value of 0.1 mGal was selected, furthermore, field data from a staggered mesh is used to help the algorithm determine perturbation [20].

## 4. RESULTS AND DISCUSSION

### 4.1 Synthetic Studies

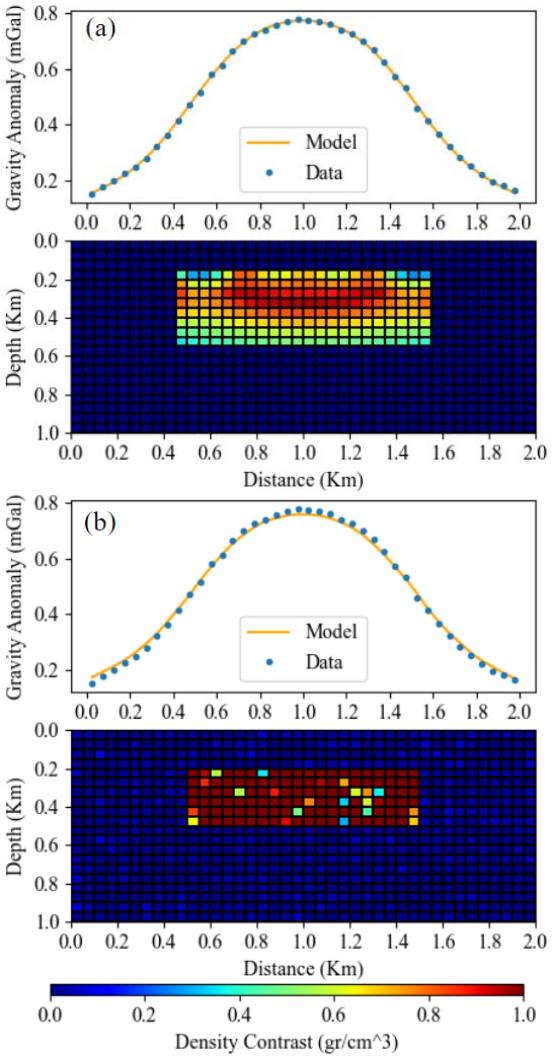


Fig. 2 LM (a) and SA (b) synthetic horizontal block model inversion with specific geological information.

Inversion modeling was carried out for 3 types of synthetic models, namely horizontal block, vertical block and fault models which have dimensions of 2 x 1 km with a mesh size of 50 x 50 m and station spacing of 50 m. The horizontal block model has anomalous object dimensions of 500 m to 1500 m on the x-axis and 200 m to 500 m on the z-axis. The vertical block model has anomalous object dimensions of 800 m to 1200 m on the x-axis and 200 m to 900 m on the z-axis. The fault model from [3] has anomalous object dimensions of 200 m to 1750 m on the x-axis and 200 m to 1000 m on the z-axis. A density contrast value of 1 g/cm$^3$ is given for anomalous objects and 0 g/cm$^3$ for the background. The synthetic gravity response is given normally distributed noise with a standard deviation of ± 0.03 mGal. The damping parameter (LM) and initial temperature (SA) were used at a value of 10-0.1 which was tuned a priori.

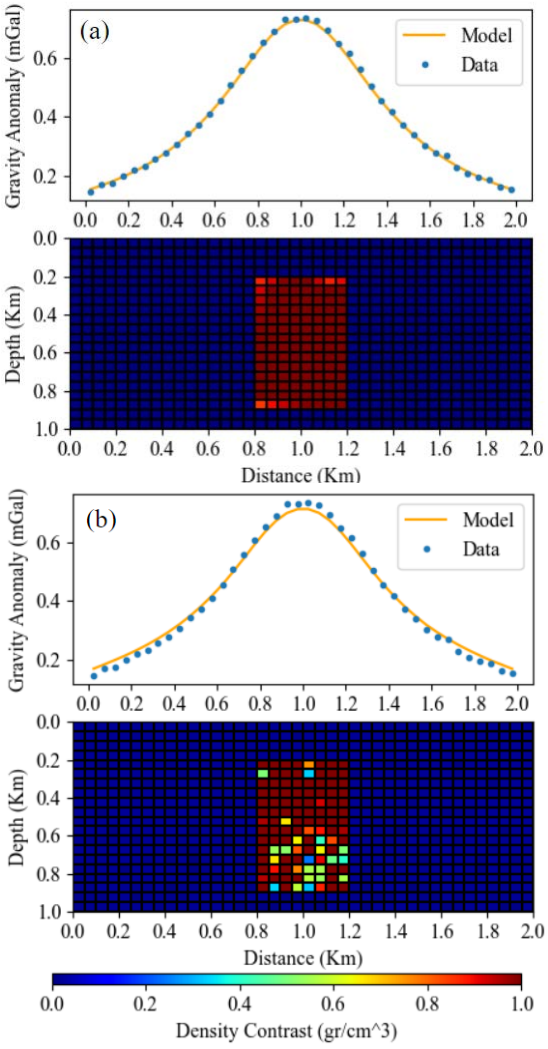


Fig. 3 LM (a) and SA (b) synthetic vertical block model inversion with specific geological information.

The synthetic model inversion result is shown in Fig. 2, Fig. 3, and Fig. 4. For the synthetic study, initial damping of 0.001 was used for LM and an initial density contrast model of 0 g/cm3 was used

for all meshes. Fig. 2., Fig. 3, and Fig. 4 shoshowat there is a slight deviation in the geometry of the model in either the LM or SA algorithm (± 700 m) especially in the horizontal block model and the fault model, but from each model, a good geometric correlation value with the synthetic model (82%-96%) is produced. From this, it can be considered that both algorithms produced a fairly good model in terms of anomaly geometry. With the given specific geometry information, the average RMSE is 0.03 mGal for the LM model and 0.12 mGal for the SA model. Inversions with minimum geometric information have also been carried out, the average RMSE was 0.03 mGal for LM and 1.08 mGal for SA. Meanwhile, the average correlation value with the synthetic model is 63% for LM and 27% for SA.

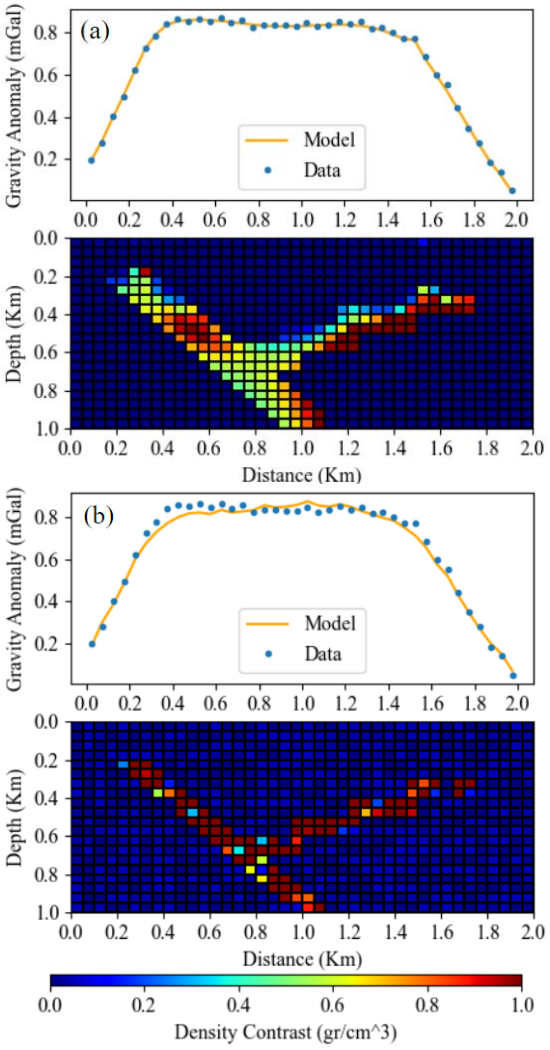


Fig. 4 LM (a) and SA (b) synthetic fault model inversion with specific geological information.

The RMSE values and correlations from the LM and SA algorithm are shown respectively in Table 1 and Table 2. With the variation of specific and minimum geometric information, it can be stated that the Levenberg-Marquardt (LM) algorithm produces an average RMSE value and correlation which is better (RMSE: 0.03 and correlation: 76%) than the simulated annealing (SA) algorithm (RMSE: 0.6 and correlation: 61%) on synthetic data. The SA algorithm is considered to be very dependent on its geometric information so that an appropriate initial guess model is needed from the field data to produce a good model, while the LM algorithm is considered more stable from the influence of geometric information. From a computational, the LM algorithm takes ± 0.5 seconds to perform 1 iteration, while within ± 0.5 seconds, the SA algorithm can produce > 1000 iterations. SA shows more effiefficiencycomputing because it does not include large matrix operations in the model perturbation.

Table 1. RMSE and Correlation Value of Levenberg-Marquardt

| Model | Levenberg-Marquardt | | | |
|---|---|---|---|---|
| | RMSE (mGal) | | Correlation | |
| | Specific | Minimum | Specific | Minimum |
| Horizontal Block | 0.05 | 0.05 | 85% | 81% |
| Vertical Block | 0.02 | 0.02 | 99% | 82% |
| Fault | 0.03 | 0.01 | 82% | 26% |
| Average | 0.03 | 0.03 | 89% | 63% |
| | 0.03 | | 76% | |

Table 2. RMSE and Correlation Value of Simulated Annealing

| Model | Simulated Annealing | | | |
|---|---|---|---|---|
| | RMSE (mGal) | | Correlation | |
| | Specific | Minimum | Specific | Minimum |
| Horizontal Block | 0.12 | 1.52 | 98% | 37% |
| Vertical Block | 0.16 | 1.52 | 97% | 23% |
| Fault | 0.07 | 0.20 | 92% | 21% |
| Average | 0.12 | 1.08 | 96% | 27% |
| | 0.60 | | 61% | |

### 4.2 Field Data Studies

The implementation of the inversion scheme to real data was conducted by applying the scheme to Mount Ungaran geothermal field gravity data. An integrated study was conducted on Bouguer anomaly data and geological data to produce accurate anomaly source information.

Ungaran is at the Eastern end of North Serayu and is a transition from the North Serayu Mountains in Central Java and the Kendeng Mountains in East Java, Indonesia. This area consists of 2 types of rock ages, namely quaternary and tertiary. Quaternary

rocks are composed of lava, andesite, breccia, and basalt, while tertiary rocks are composed of conglomerate, clay, sandstone, marl, volcanic breccia, and limestone [15].

The residual anomaly value is obtained by applying the upward continuation method to the Bouguer anomaly and visualized into a kriging contour in Fig. 5. The high anomaly zone which has a value of 9 mGal to 13 mGal, is located in the north and south of the study area and is thought to be associated with high-density andesite-basalt rocks.

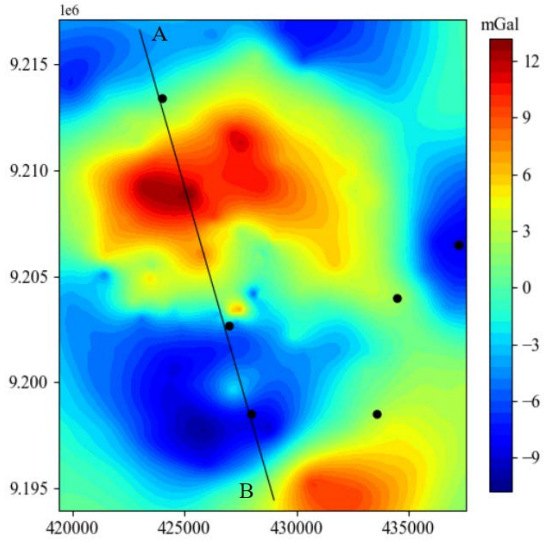


Fig. 5. Residual anomaly contours, black circles indicate the location of geothermal manifestations and black lines respectively modeling line profile from A to B.

The moderate anomaly zone which has a value of 0 mGal to 6 mGal located in the southeast and continues to the west of the study area, whereas the low anomaly zone which has a value below 0 mGal is in the northern corner continuously to the east, and southwest of the study area. Moderate and low anomalous zones are thought to be associated with Young Quaternary rocks composed of lava. Moreover, the interpretation of the Ungaran Bouguer anomaly is based on the density and silica content of the Ungaran rock sample. It was concluded that high anomaly values were associated with high-density Old Ungaran, while low anomalies were thought to be associated with low-density Young Ungaran [19][21].

Spectrum analysis on Bouguer anomaly data was carried out to estimate the depth of anomaly objects. The estimated depth of deep-seated objects is 5039.4 meters, whereas for shallow objects is 466.8 meters. From this information, it can be determined that the depth limit of the inversion model will refer to the depth of deep-seated objects, which is ± 5000 meters.

The profiling line for modeling shown in Figure 5 is made to the Northwest – Southeast to cross the geological structure and geothermal manifestations in Ungaran. Furthermore, the first horizontal derivative (FHD) method is applied to the profile trajectory to determine the horizontal boundaries of anomalous objects in the research field. FHD in this study was conducted in the spatial domain and produces a curve shown by a red line in Fig. 6, while the residual anomaly is shown by a blue line. The horizontal boundaries of the anomalous objects are interpreted to be located at coordinates 6000 m and 13500 m on the x-axis of the graph. peak FHD is assessed as a representation of the horizontal boundary of a large, high-density object, namely igneous rock intrusion, this object is thought to be part of old Ungaran.

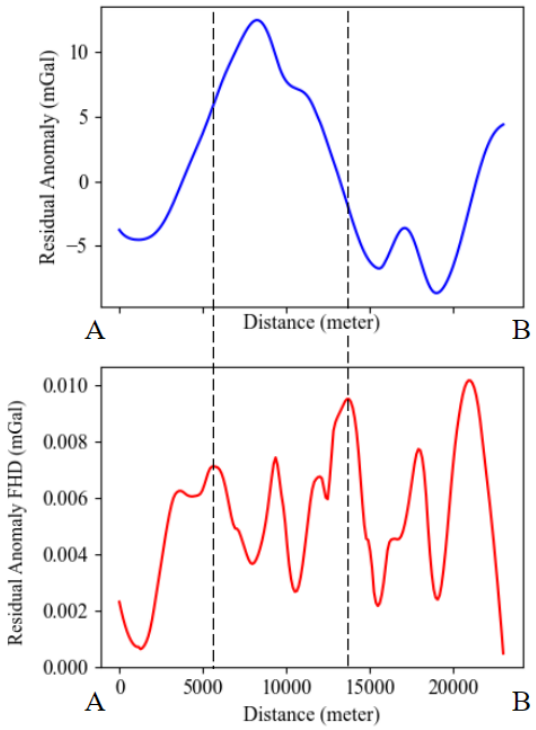


Fig. 6. Residual anomaly profile (top) and first horizontal derivative (FHD) profile (bottom), black dashed lines indicate the interpreted anomaly boundaries.

An initial guessed model with a density of 0 g/cm3 for the inversion process is shown in Fig. 7. Staggered mesh which varies vertically and horizontally is used [20]. This variation refers to the results of the analysis of the first horizontal derivative which gets the horizontal limit at a position of 6000 m to 13500 m on the x-axis and the depth limit of the model from spectrum analysis which is 5000 m. In this study, the Levenberg-Marquardt (LM) inversion algorithm was used with an initial damping parameter of 0.1 and a change of

1%. The limitation of the density contrast value with a maximum limit of 0.3 g/cm$^3$ and a minimum limit of -0.2 g/cm$^3$ based on rock lithology information [15] is also included.

The results of the Levenberg-Marquardt inversion are shown in Fig. 8. After 61 iterations with a computation time of ± 17 seconds, a model with an RMSE value of 0.001 mGal was obtained. Based on the RMSE value, it can be considered that the Levenberg-Marquardt algorithm is very good at real data inversion. The disadvantage of this algorithm is the influence of determining the initial damping parameter on the inversion convergence. If the determination of the initial damping parameters is optimum, the algorithm will be faster to arrive at the best solution.

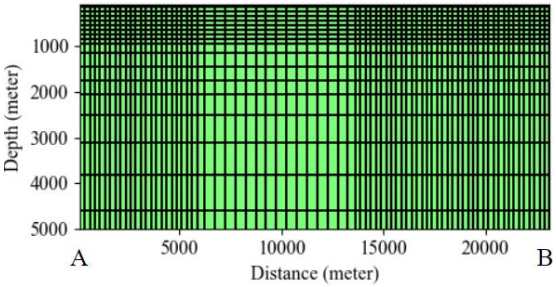


Fig. 7. An initial guessed model with staggered mesh

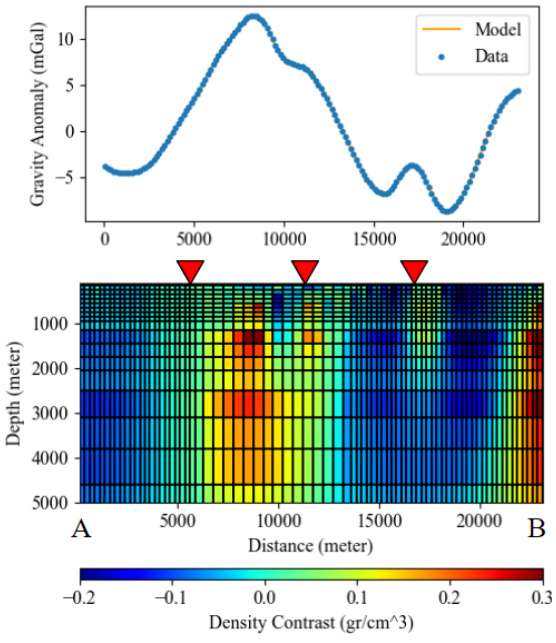


Fig. 8. Levenberg-Marquardt Ungaran inversion model. The red triangle indicates geothermal manifestations

The RMSE value for the iterations is shown in Fig. 9. It can be stated that the selection of the initial damping value and its changes was quite optimum based on the smoothness of the curve and the RMSE value which was close to zero before the 10th iteration.

The results of the simulated annealing inversion are shown in Fig. 10. Simulated Annealing (SA) inversion was carried out with an initial temperature parameter of 10 and a decrease of 0.99. The perturbation model space is divided into 3, namely high density, medium density (background), and low density. This model space is created a priori and tuned to get the best model. The limitation on the density contrast value with a maximum limit of 0.3 g/cm3 and a minimum of -0.2 g/cm$^3$ is used.

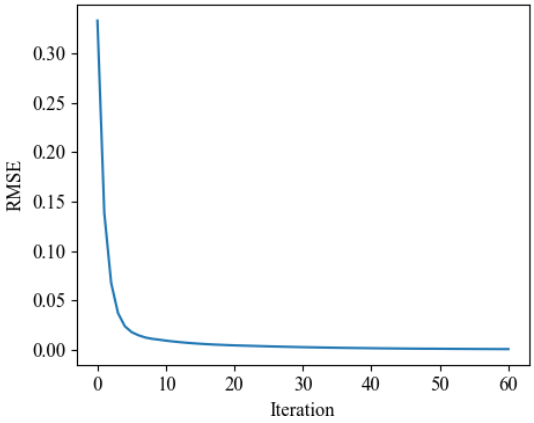


Fig. 9. RMSE vs iteration curve of Levenberg-Marquardt Ungaran inversion model

The results of the simulated annealing inversion are shown in Fig. 10. Simulated Annealing (SA) inversion was carried out with an initial temperature parameter of 10 and a decrease of 0.99. The perturbation model space is divided into 3, namely high density, medium density (background), and low density. This model space is created a priori and tuned to get the best model. The limitation on the density contrast value with a maximum limit of 0.3 g/cm3 and a minimum of -0.2 g/cm$^3$ is used.

The best model with an RMSE value of 0.7 mGal was obtained after reaching 13811 iterations and a computation time of ± 7 seconds. Based on the selected misfit tolerance value for field data, which is 0.1 mGal, it can be considered that the SA algorithm made in this study is not good enough for field data. This is presumably because this algorithm has a considerable influence on the a priori determination of computational parameters (initial temperature, model space) [12]. The level of the geometric complexity of field anomalies is also thought to affect the results of this inversion, whereas, in previous studies using the SA algorithm [13][22][23], the target model was a sedimentary model that its geometry is considered more uniform than the Ungaran volcanic model. The RMSE value against the iterations is shown in Fig. 11. The resulting iteration process towards the minimum

RMSE value (convergent) starts at iterations > 700, then starts to approach 0 at iterations > 10000.

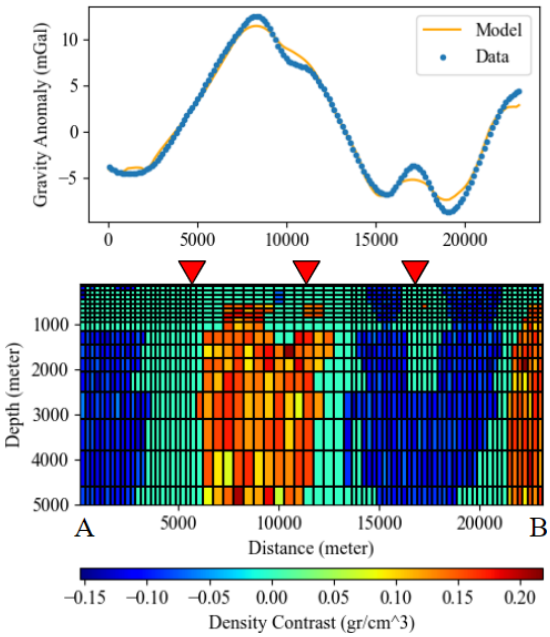


Fig. 10. Simulated annealing Ungaran inversion model. The red triangle indicates geothermal manifestations

In the LM model, the high-density contrast is 0.2-0.3 g/cm$^3$, while in the SA model, the high-density contrast is 0.15-0.22 g/cm$^3$. High density at 6000-13500 meters on the x-axis is interpreted as andesite intrusion. Meanwhile, for high density at a position of 21000-23000 meters on the x-axis, it is interpreted as an old quaternary rock with an andesite composition. For low-density contrast, the LM model is -0.1 to -0.2 g/cm$^3$, while the SA model is -0.1 to -0.15 g/cm$^3$.

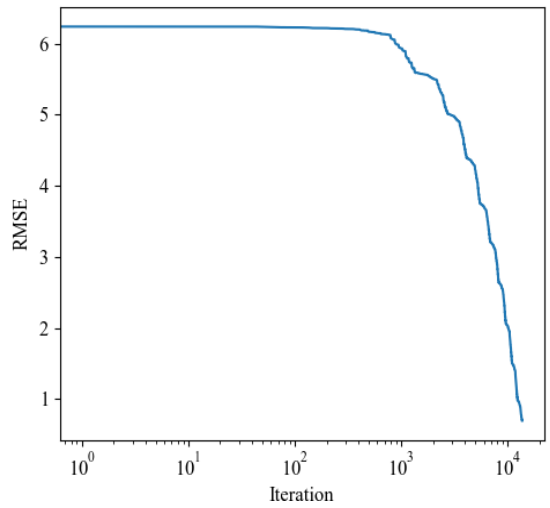


Fig. 11. RMSE vs iteration curve of simulated annealing Ungaran inversion model

The low density is interpreted as a young quaternary rock composed of andesite lava [19]. The density contrast value produced is also assessed to be correlated with the appearance of geothermal manifestations on the surface. The absolute density value can be calculated from the density contrast of the two models, the high density is 2.89-2.99 g/cm$^3$ (LM) and 2.84-2.91 g/cm$^3$ (SA), and the low density is 2.49- 2.59 g/cm$^3$ (LM) and 2.54-2.59 g/cm$^3$ (SA). The subsurface model was found to be correlated with the model produced in previous studies by [19], [24], and [25] based on model geometry and density values.

## 5. CONCLUSION

Based on the inversion of synthetic data, the average RMSE value was 0.03 mGal with a correlation of 76% for the Levenberg-Marquardt (LM) algorithm and an average RMSE of 0.6 mGal with a correlation of 61% for the simulated annealing (SA) algorithm. Based on the inversion of field data, the RMSE value is 0.001 mGal for the LM algorithm and 0.7 mGal RMSE for the SA algorithm. Overall, the Levenberg-Marquardt algorithm is considered to be better and more stable in producing subsurface density models. The Levenberg-Marquardt (LM) and simulated annealing (SA) algorithms both produce models that represent old Ungaran rocks with a density of 2.89-2.99 g/cm$^3$ (LM) and 2.84-2.91 g/cm$^3$ (SA), and young Ungaran with a low density of 2.49-2.59 g/cm$^3$ (LM) and 2.54-2.59 g/cm$^3$ (SA).

## 6. REFERENCES

[1] Supriyanto, Geophysical Data Analisis: Understanding Inversion Theory, Department of Computational Physics Universitas Indonesia, 2007, pp. 1-34. (In Indonesian).

[2] Bear G.W., Al-Shukri H.J., and Rudman A.J., Linear Inversion of Gravity Data for 3-D Density Distributions, Geophysics, Vol. 60, issue 5, 1995, pp. 1354-1364.

[3] Grandis H., Introduction to Geophysical Inversion Modelling, Association of Indonesian Geophysicists, 2009, pp. 105-113. (In Indonesian).

[4] Said U., Heriyanto M., and Srigutomo W., Comparision of Least-Square Inversion with Levenberg-Marquardt on Geomagnetic Method for Crustal Block Model, Proceedings SKF, 2016, pp. 433-440. (In Indonesian).

[5] Levenberg K., A Method for The Solution of Certain Non-linear Problems in the least Squares, Quarterly of Applied Mathematics, Vol. 2, no. 2, 1944, pp. 164-168.

[6] Widodo and Saputera D.H., Improving Levenberg-Marquardt Algorithm Inversion Result Using Singular Value Decomposition, Earth Science Research, Canadian Center of Science and Education, Vol. 5, No. 2, 2016, pp. 20-31.
[7] Marquardt D.W., An Algorithm for Least-Squares Estimation of Nonlinear Parameters, Journal of The Society for Industrial and Applied Mathematics, Vol. 11, No. 2, 1963, pp. 431-441.
[8] Arroyo O.J.C., Jones J.M.R., and Treviño E.G., Robust Estimation of Temporal Resistivity Variations: Changes From The 2010 Mexicali, Mw 7.2 Earthquake and First Results Of Continuous Monitoring, Vol. 72 2018, pp. 288-300.
[9] Wijaya R., Bahri A.S., and Warnana D.D., 1-D Inversion Difference Analysis Occam and Simulated Annealing Methods on Magnetotelluric Data, Jurnal Teknik ITS, Vol. 2, No. 2, 2016, pp. B355-B358. (In Indonesian).
[10] Kirkpatrick S., Gelatt C.D., and Vecchi M.P., Optimization by Simulated Annealing, Science, Vol. 220, Issue 4598, 1983, pp. 671-680.
[11] Chunduru R.K., Sen M.K., Stoffa P.L., and Nagendra R., Non-Linear Inversion of Resistivity Profiling Data for Some Regular Geometrical Bodies, Geophysical Prospecting, Vol. 43, No. 8, 1995, pp. 979-1003.
[12] Biswas A., Interpretation of Gravity and Magnetic Anomaly Over Thin Sheet-Type Structure Using Very Fast Simulated Annealing Global Optimization Technique. Modeling Earth Systems and Environment, Vol. 2, No. 30, 2016, pp. 1-12.
[13] Netto A. and Dunbar J., 3-D Constrained Inversion of Gravimetric Data to Map The Tectonic Terranes of Southeastern Laurentia Using Simulated Annealing, Earth and Planetary Science Letters, Vol. 513, 2019, pp. 12-19.
[14] Blakely R.J., Potential Theory in Gravity and Magnetic Applications, Cambridge University Press, 1995, pp. 214-218.
[15] Thanden R.E., Sumadirdja H., Richards P.W., Sutisna K., and Amin T.C., Geology Map of Magelang and Semarang Java Sheet Scale 1: 100000, Geological Research and Development Center, 57, 1996, (In Indonesian).
[16] Barbosa V.C.F. and Silva J.B., Generalized Compact Gravity Inversion, Geophysics, Vol. 59, No. 1, 1994, pp. 57-68.
[17] Chai T., Draxler R.R., Root Mean Square Error (RMSE) or Mean Absolute Error (MAE)? – Arguments Against Avoiding RMSE in The Literature, Geoscientific model development, Vol. 7, No. 3, 2014, pp. 1247-1250.
[18] Obilor E.I. and Amadi E.C., Test for Significance of Pearson's Correlation Coefficient, International Journal of Innovative Mathematics, Statistics & Energy Policies, Vol. 6, No.1, 2018, pp. 11-23.
[19] Setyawan A., Ehara S., Fujimitsu Y., Nishijima J., Saibi H., and Aboud E., The Gravity Anomaly of Ungaran Volcano, Indonesia: Analysis and Interpretation, Journal of the Geothermal Research Society of Japan, Vol. 31, Issue 2, 2009, pp. 107-116.
[20] Arato A., Gadio A., and Sambuelli, Staggered Grid Inversion of Cross Hole 2-D Resistivity Tomography, Journal of Applied Geophysics, Vol. 104, 2014, pp. 60-70.
[21] Setyawan A., Yudianto H., Nishijima J., and Hakim S., Horizontal Gradient Analysis for Gravity and Magnetic Data Beneath Gedongsongo Geothermal Manifestations, Ungaran, Indonesia, Proceedings World Geothermal Congress, 2015, pp. 1-6.
[22] Nagihara S. and Hall S.A., Three-Dimensional Gravity Inversion Using Simulated Annealing: Constraints on The Diapiric Roots of Allochthonous Salt Structures, Geophysics, Vol. 66, No. 5, 2001, pp. 1438-1449.
[23] Roy L., Sen M.K., Blankenship D.D., Stoffa P.L., and Richter T.G., Inversion and Uncertainty Estimation of Gravity Data Using Simulated Annealing: An Application Over Lake Vostok, East Antarctica, Geophysics, Vol. 70, No. 1, 2005, pp. J1-J12.
[24] Saibi H., Aboud E., Setyawan A., Ehara S., and Nishijima J., Gravity Data Analysis of Ungaran Volcano, Indonesia, Arabian Journal of Geosciences, Vol. 5, No. 5, 2012, pp. 1047-1054.
[25] Utami R.R., Setyawan A., and Gernowo R., Interpretation of Subsurface Structure of Gravity Data Using Artificial Neural Network Algorithm Case Study of Ungaran Geothermal Area Central Java, Youngster Physics Journal, Vol. 5, No. 4, 2016, pp. 373-380.